891. Large structural impact localization based on multi-agent system

Dong Liang[1], Shenfang Yuan[2], Lei Qiu[3], Schmicker David[4], Jian Cai[5], Menglong Liu[6]
[1, 2, 3, 4, 5, 6]The Aeronautic Key Laboratory of Smart Materials and Structures
Nanjing University of Aeronautics and Astronautics 241#
29# Yu Dao Street, Nanjing 210016, People's Republic of China
[4]Faculty of Mechanical Engineering, Otto von Guericke University of Magdeburg
University Square 2, Magdeburg 39106, Germany
[2]Corresponding author
E-mail: [1]*ld19821213@126.com*, [2]*ysf@nuaa.edu.cn*

(Received 09 August 2012; accepted 4 December 2012)

Abstract. In practical applications of structural health monitoring, a huge amount of distributed sensors are usually used to monitor structures of large dimensions. In order to obtain fast and accurate evaluation of a structure, a multi-agent system is introduced to manage different sensor sets and to fuse distributed information. In this paper, a multi-agent system based on impact location is presented to deal with the impact load localization problem for large-scale structures. The monitoring system firstly detects whether an impact event happens in the monitored sub-region, and focuses on the impact source on the sub-region boundary to obtain the sensor network data with blackboard systems. Then the collaborative evaluation of both the acoustic emission and the inverse analysis localization method is employed to obtain precise and fast localization result. Finally, a reliable assessment for the whole structure is provided by fusing evaluation results from the sub-regions. The performance of the proposed multi-agent system is illustrated by means of experimental on a large aerospace aluminum plate structure. Extensive testing of the proposed system demonstrated its effectiveness for the impact load localization in each sub-region, particularly for impacts lying next to the borders of the sub-regions.

Keywords: structural health monitoring, multi-agent system, impact location, sensor network, blackboard system, coordination evaluation, large structures.

1. Introduction

Structural health monitoring (SHM) is a field of research that is addressed by many engineering and academic teams at present. It utilizes advanced sensor and actuator devices integrated in the structural material with aim to execute a wide range of real-time online monitoring tasks. Recently, composite materials are increasingly used in aircraft primary structures (B787, Airbus A380, F35, Typhoon) because of their superior strength properties over metallic materials. However, low-velocity impact can cause matrix cracking, delamination and broken fibers leading to significant reduction of strength and fatigue life [1-3]. Hence, it is necessary to utilize SHM to real-time monitor the impact incidents and localize their spots. At present, a number of methods have been applied to estimate the impact location. There are mainly the acoustic emission (AE) method and the inverse analysis method in the impact localization research. For the widely used AE technology, most of the significant research efforts have focused upon the impact localization inside the monitored area, while hardly any reports take the impact location related to the region boundary into account because of the unsatisfactory localization. For the large structure, the impact may occur at any position, and the region boundary monitoring is also very important. Furthermore, the model error of the inverse analysis method affects the impact location accuracy largely although it does not relate to the position. Meanwhile, the computation time of the AE method is significantly lower than the one of the inverse analysis method. Therefore, for the large structures, there is no a kind of precise and real-time impact load localization in these methods. It is still a large and challenging

task to monitor the impact events precisely and fast in the actual large-scale structure. In order to solve the problem, multi-agent system (MAS) is adopted to coordinate and manage distributed sensor networks, fuse information from different sensors, and take advantage of different estimation methods. In artificial intelligence (AI), MAS has been a natural model for developing a large-scale, complex, distributed system, which is loosely coupled and heterogeneous. It is an effective way for solving large-scale distributed problem [4].

At present, MAS has been adopted for fault diagnosis and health monitoring, and there are some reports on MAS related to mechanical fault diagnosis and health monitoring, etc.

In fault diagnosis domain, Stephen D. J. worked at the research and the application of multi-agent power system condition monitoring [5]. NASA's Lyell, etc analyzed and designed the International Space Station electric power system health monitoring system using MAS and provided the simulation [6]. For fault detection and identification in chemical processes, Yew Seng Na utilized MAS to fuse different FDI methods for eliminating the results conflict and improving the diagnosis performance [7]. Their research focused on the construction of a single monitoring agent, the design and the functional verification of MAS for their fields.

In SHM domain, research on MAS is in the initial stages. Since 2002 NASA's Science and Technology Information Program (STI) made a research on non-life aerial vehicles using self-agent theory, and the work focused on the coordinate research of MAS [8]. Albert Esterline, Bhanu Gandluri, etc. put forward MAS for the vehicle health management system, and their research was the distributed problem-solving based on contract net protocol [9]. Subsequently, Albert Esterline improved the above work and implemented MAS using JADE platform [10]. Shenfang Yuan initially proposed the distributed SHM system based wireless sensors and MAS, which gave the agent's basic definition and implementation (Yuan et al., 2006). Then, Xia Zhao, Shenfang Yuan, etc. presented a complete design method for SHM system based on MAS (SHM MAS) including ontology design, distributed database realization, facilitator design and introduced the validation work of the case study in a large aviation aluminum plate in detail [11-13].

In our past work, SHM MAS is utilized for the localization of impact loads on structures [13]. Therein, the diagnostic agent is actually an expert system, and is adopted to monitor the impact event for different materials. However, it does not consider how PZT sensors are managed and how the kinds of impact damage evaluation methods are coordinated for accurately and real-time localization in the whole large complicated structure. To solve the problem, this paper presents a SHM MAS for the impact location, and gives the system implementation and experimental verification. In the MAS, the blackboard system is applied to manage geographically distributed PZT sensor networks to obtain the effect data about the impact load inside the monitored region or on its boundary, and to coordinate and fuse the AE method and the inverse analysis method to locate the impact load precisely and fast.

The rest of this paper is structured in the following manner. Section 2 introduces the framework of SHM MAS. Section 3 presents SHM MAS evaluation of the impact location. In Section 4, SHM MAS experimental verification is provided. Finally, Section 5 concludes the paper.

2. Development of structural health monitoring system based on multi-agent system

The SHM architecture based on MAS presented [12] is shown in Fig. 1. A MAS has been developed to aid in the SHM [13]. Considering a typical SHM system, a large-scale structure can be divided into several subareas monitored. The sensors are placed in or on the structure to acquire the data on the structural status parameters. The appropriate signal or information processing methods are used to analyze and extract the damage-sensitive features from the sensing data. The corresponding damage evaluation methods can obtain the structure health status using the key feature. Thus, according to three typical parts, three layers can be defined to

form SHM MAS. They are data monitoring layer, data interpretation and damage diagnostic layer. Considering a large-scale structure divided into some subareas, an information layer is needed to fuse the damage information from the local subareas and provide the whole information to the user.

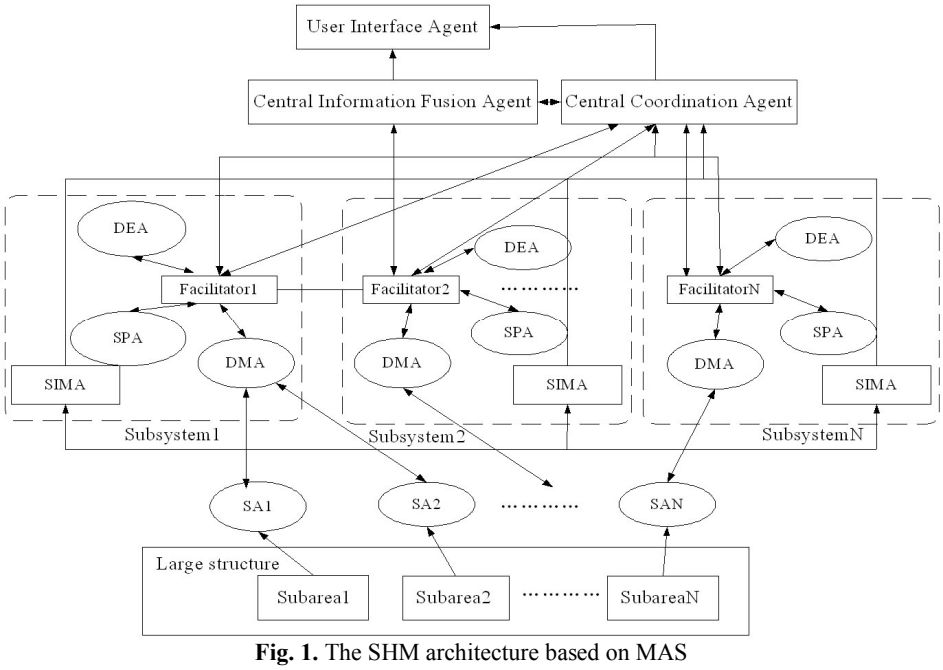

Fig. 1. The SHM architecture based on MAS

Data monitoring layer includes sensing agent (SA) and district monitor agent (DMA). The data interpretation and the damage diagnostic layer separately correspond to signal processing agent (SPA) and damage evaluation agent (DEA). The information fusion layer is realized by facilitator agent (FA), central coordination agent (CCRA), central information fusion agent (CIFA), user interface agent (UIA) and sharing information management agent (SIMA). DMA manages several SAs and obtains the important damage data in local area. In every subsystem, FA provides "yellow pages" services to every kind of agent. It is in charge of registering and managing every agent service, such as feature extraction and damage assessment. Thus this is convenient for the agent to search the services and resources to achieve interaction and collaboration. CCRA is responsible for the coordination among subsystems, such as conflict solving, time synchronization, resource distribution and negotiation strategy etc. CIFA fuses the damage information from different subareas to give a global estimation of the whole structure. UIA provides information to the user and accepts the user's instruction. In every subsystem, SIMA is a distributed database, and it allows the agent to publish its identity (ID) and address in order that other agents can easily find it, and it is beneficial to exchange the information between different DEAs in the same or different subsystems. Meanwhile, it saves and provides the DEA's parameter. The social ability and co-operation between the agents leads to the final damage estimation of the complete structure.

3. Evaluation of impact location based on multi-agent system

In the paper, SHM MAS evaluation for the impact location is introduced through a case study. Taking advantages of MAS, this SHM system for the impact location should demonstrate

the following functions: the system can focus on the impact load in the area or close to the boundary, and coordinate and fuse different types of damage evaluation methods to obtain the fast and precise results. The following sections provide a detailed description of SHM MAS for the impact location.

3. 1. System setup

In this work, a large aerospace aluminum plate structure as the evaluation object is studied using MAS. In Fig. 2 and 3 the structure and the sensor layout diagram, and the photo of the structure are given. The structural material is the aerospace hard aluminum LY12. Its basic dimensions and material properties are listed in Table 1. The 64 M6-bolts are deployed around the structure with the distance of 10 cm, and are used to fix the plate with bracket. The bracket is put on the ground vertically, supporting the aluminum structure. The structure is divided into eight sub-regions, each of which is 49 cm × 45 cm except its edge. A strain network is utilized to measure strain responses, in which the PZT sensors with 0.8 cm diameter and 0.04 cm thickness are laid on the vertices of each sub-region. In addition, each subarea is divided into nine regional units.

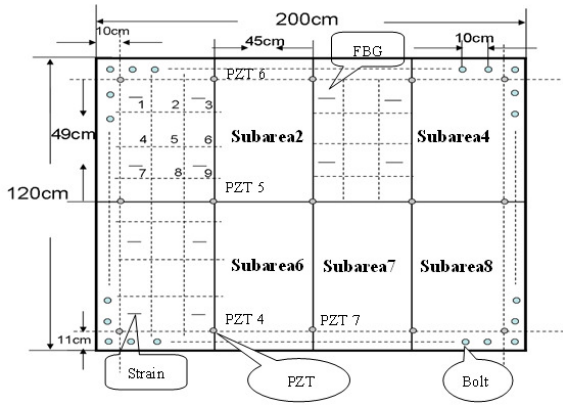

Fig. 2. System setup

Fig. 3. The picture of the aluminum plate and sensor distribution

As shown in Fig. 3, the system consists of a large aerospace aluminum plate specimen, an impact hammer, a data acquisition system and an industrial control computer.

Table 1. Specimen properties

Aluminum	
Geometry (rectangular) Length Width	 200 cm 120 cm
Thickness	0.25 cm
Modulus of elasticity Poisson's ratio Density	71.7 Gpa 0.33 2.778 g/cm^3

3. 2. Multi-agent development

SHM MAS comprises data monitoring layer agents, data interpretation layer agents, damage diagnostic layer agents and information layer agents. Each of the layers contains a number of agents performing different functions. The functionality and major composition principles of the agent within each layer are described below.

SA is implemented by hardware and software, and the other agents are only implemented by software. The software is programmed with Labview 8.5 and Matlab R2006a in the industry control computer.

(1) Data monitoring layer agents

PZT sensing agent (PZT SA): The agent is responsible for measuring the strain response of the structure subarea and judging whether the impact occurs in the subarea.

In the assessment, each PZT SA consists of four piezoelectric sensors in a monitored subarea, four charge amplifiers, a multi-channel digital trigger circuit, a quad-channel data acquisition card, controlled by Labview software, which includes the acquisition, communication and self-monitoring program. The structure diagram is shown in Fig. 4. There are two shared sensors for two neighboring PZT SAs. PZT Sensor 1 to 9 is used to monitor the impact event occurring in multi-regions.

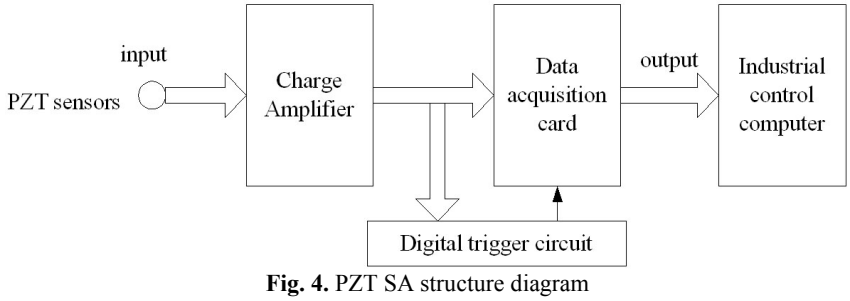

Fig. 4. PZT SA structure diagram

Nine sensor responses due to the applied impact are amplified through the charge amplifiers (Yangzhou Electric Company, YE5853) as shown in Fig. 5. The multi-channel digital trigger receives the output signal from the charge amplifier. Its circuit schematic diagram is shown in Fig. 6. The quad voltage comparator LM239 is used, which includes four operational amplifiers. TC4072BP/BF integrates two positive logic OR gates with four inputs. A/D conversion is conducted through quad-channel data acquisition card (National Instrument Company, PCI-6115). Three data acquisition boards are linked with RTSI bus cables as shown in Fig. 7. They are synchronously triggered by multi-channel digital trigger, and acquire the voltage signal of the charge amplifier. Finally, strain responses are transmitted to the computer with PCI bus.

District monitor agent (DMA): The agent uses a blackboard system to manage four neighboring PZT SAs, focuses upon the region in which the impact happens, and gets the valid data. It is implemented with a work thread integrating with the blackboard structure and the communication protocol interaction thread.

(2) Data interpretation layer agents

The layer agents have the work threads integrating with the Matlab function, and the communication protocol interaction thread, and their tasks are to extract the main frequency and the arrival time difference of the signal.

Fast Fourier transform signal processing agent (FFT SPA): The agent implements the frequency spectral analysis of the strain data from PZT SA, and derives the main frequency, which is chosen as the center frequency of the wavelet analysis.

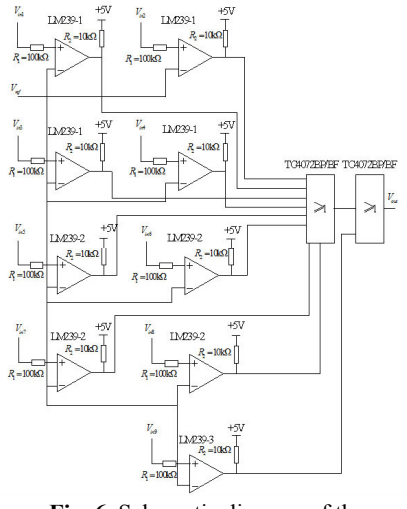

Fig. 6. Schematic diagram of the digital trigger circuit

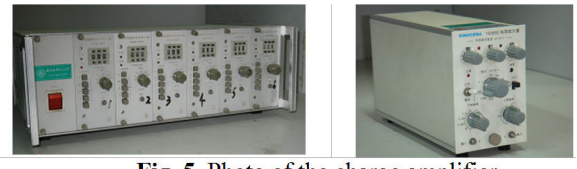

Fig. 5. Photo of the charge amplifier

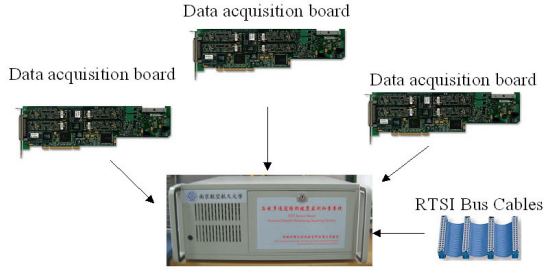

Fig. 7. Photo of the acquisition system

Wavelet transform signal processing agent (WT SPA): The agent subscribes the main frequency from FFT SPA as the center frequency of Gabor wavelet, and applies the wavelet transform [14] to implement the time-frequency analysis of dispersive plate waves related to the signals collected by PZT SA. As a result, the arrival time of the wave group velocity is extracted, which is adopted to identify the exact location of the impact event.

(3) Damage diagnostic layer agents

The principles of the AE and the inverse analysis method are given below in detail. The layer agents also consist of the work thread integrating with the Matlab function, and the communication protocol interaction thread in charge of computing the impact position.

Triangulation localization damage estimation agent (TL DEA): For the agent, the time delays between three sensors in the subarea are adopted to estimate the impact position as shown in Fig. 8 [15]. Assume the AE source occurs at the location $A(x, y)$, S_{ij} is the distance between sensor i and j, l_i is the distance between the impact source and sensor i, and θ_i is the angle defined in figure, $i, j = 1,2,3$. The arrival time difference Δt_{ij} between two sensors is easily derived with the wave propagation time from the impact source to PZT sensor 1, 2, 3. By finding the arrival times to each sensor for frequency f, one can find:

$$\begin{aligned}\Delta t_{12}(f) &= t_1(f) - t_2(f) = \frac{l_1}{C_{g_1}(f)} - \frac{l_2}{C_{g_2}(f)} \\ \Delta t_{23}(f) &= t_2(f) - t_3(f) = \frac{l_2}{C_{g_2}(f)} - \frac{l_3}{C_{g_3}(f)}\end{aligned} \quad (1)$$

where $C_{g_i}(f)$ is the wave velocity on the direction from impact source to sensor i. Also, with the triangle geometry relation between the impact position and sensors, we know:

$$\begin{aligned} l_1 \sin\theta_1 &= l_2 \sin\theta_2 \\ l_1 \sin\theta_1 + l_2 \sin\theta_2 &= S_{12}\end{aligned} \quad (2)$$

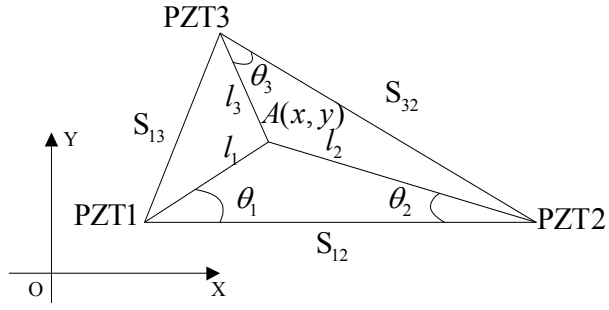

Fig. 8. Diagram of triangulation method

By solving the above set of nonlinear Equation (1) and (2), θ_1, θ_2 can be found, from which the coordinate (x, y) of location A can be determined for each frequency f.

The aluminum is isotropic material, so the acoustic emission source propagates with equal speed in the plate, and the impact location is easily resolved.

Inverse analysis localization damage estimation agent (IAL DEA): The agent uses the inverse analysis method in time domain [16, 17] to identify the impact location by minimizing the relative error between the numerical strains and experimental ones from PZT SA.

In the research, the inverse analysis method in time domain for the impact localization is taken [18], which is based on the optimized identification of impact force with Chebyshev polynomial basis function. The structural finite element model is adopted to obtain the modal frequency and the modal vector. With the modal superposition principle, the plate vibration equation and the measurement strain are adopted to build the optimization model for identifying the impact force and location.

Assuming N PZT sensors and considering L discrete time points t_1, t_2, ..., t_L within the time domain [0, T], for the ith sensor, the computational strain function vector and the measurement strain vector at these time points are $\varepsilon_i = [\varepsilon_i(t_1),\ \varepsilon_i(t_2),\ ...,\ \varepsilon_i(t_L)]$ and $\varepsilon_i^* = [\varepsilon_i(t_1),\ \varepsilon_i(t_2),\ ...,\ \varepsilon_i(t_L)]$. Consequently, the optimal model is:

$$\min_{\eta} \sum_{i=1}^{N} \left\| \varepsilon_i(\eta) - \varepsilon_i^* \right\|^2, \quad s.t.\ F(t) \geq 0. \tag{3}$$

By solving the above optimization model, the Chebyshev polynomial coefficient vector η is obtained, followed by construction of impact force $F(t)$.

This method assumes that impact location is known, the impact force is reconstructed. By traversing all finite element nodes on the entire structure, different impact forces are obtained, in which the impact location of the best approximation measurement strain response is the optimization solution. The optimization model on the impact location is:

$$\min_{p} \frac{\sum_{i=1}^{N} \left\| \varepsilon_i(p) - \varepsilon_i^* \right\|^2}{\sum_{i=1}^{N} \left\| \varepsilon_i^* \right\|^2} \tag{4}$$

where p is the load position vector.

(4) Information layer agents

The layer agents also integrate with the work thread and the communication protocol interaction thread.

Facilitator agent (FA): Every subsystem should host a default FA. It manages the agent ID and service name built with Labview cluster array.

Sharing information management agent (SIMA): A default SIMA should host in every subsystem, and manage all the IDs and addresses in the subsystem, and is able to start up and stop other agents. The IDs and addresses are built with Labview cluster array, and are set be shared variable.

Central information fusion agent (CIFA): Once the impact happens in the edge of two adjacent subareas, the agent fuses the damage information from neighboring subareas to provide exact location estimation with a simple fusion algorithm.

User interface agent (UIA): The agent provides information to the user and accepts the user's instruction. UIA is realized with Labview control.

Central coordination agent (CCRA): The agent is responsible for coordinating and processing the evaluation results from different subsystems according to the DMA decision. If the damage occurs near the boundary, CCRA waits and obtains two assessment results, and sends them to CIFA for information fusion. If the damage occurs in the sub-region, CCRA gets the result, and directly publishes it to UIA.

The agent management in SHM MAS for the impact location consists of three components depicted as yellow-page, white-page and life-cycle service. SIMA is responsible for the white-page and life-cycle service, maintaining a directory of agent identifiers (AID) and agent state. AID makes up of agent ID and address. The agent states adopted are "start", "suspend", "resume" and "stop". When each agent stars up, it registers with SIMA. FA then requests the agents' addresses from SIMA and queries each about what services are available.

In the study, standard agent conventions have been adopted. This means that all inter-agent communications are handled using just a few types of message, examples of which are "Subscribe", "Query-ref", "Inform", "Propose", "Publish", "Confirm", "Call for propose". Sending messages or sharing the blackboard is employed for inter-agent communication in SHM MAS.

The SHM MAS ontology is based on the content we presented [11, 12]. It contains the concept, the data attribute and the object attribute. The concept Sensor data with its data attribute is defined as follows: Sensor data (subarea ID, PZT sensor ID, sensor, static or dynamic, valid or invalid, data length, data, timestamp). Its object attribute tells us that SPA is suitable for Sensor data. For the concept Sensor data feature, its data attribute is Sensor data feature (Feature ID, data length, data, timestamp) and its object attribute is that DEA is suitable for the feature.

3. 3. Multi-agent coordination

The MAS comprises a number of agents, which is to solve the complex problem not finished by a single agent, and is the coordination network among agents. The coordination mechanism is the key issue in MAS research. In SHM MAS for the impact location, the coordination approach based on the blackboard system is applied among the sensing agents or between the evaluation agents.

A blackboard is an effective communication mode for the agent collaboration [19]. It is the system's shared database, with which the agents can exchange data, information and knowledge. It is divided into a number of information layers, which correspond to the intermediate representation of the problem and are adopted to record raw data, intermediate results and final conclusions. Therefore, it is various solutions set of problems. Each agent

monitors the state of the blackboard, and seeks the chance to solve the problem. Once the agent finds that the blackboard information can support it to further solve the problem, it begins to solve the problem, and the results are recorded in the blackboard. The new additional information is useful for the other agents to continually solve it. Repeat this process until the problem is completely resolved.

3. 3. 1. Sensing agent supervision

For each PZT SA, its self-monitoring program is adopted to determine whether the impact is in the region or other regions. In Fig. 9 the distances differences between the impact location inside the subarea and its four sensors are less than the ones between the impact location outside the subarea and sensors. Thus, for the isotropic plate or the anisotropic plate which is similar to be isotropic, whether the impact occurs in the region can be estimated using the time lag between the arrival times at which the impact signal reaches the sensors. Here, the threshold crossing method [14] is adopted to obtain the signal arrival time.

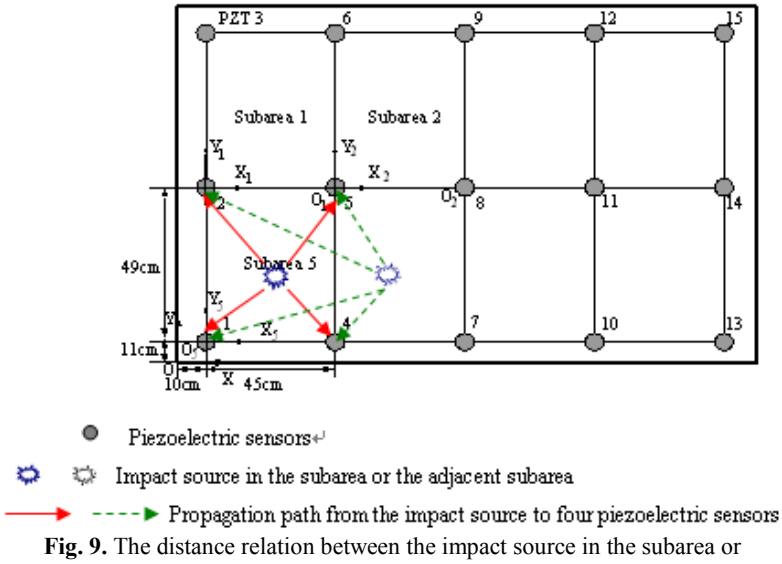

Fig. 9. The distance relation between the impact source in the subarea or the adjacent subarea and the sensor

The maximum of the arrival time differences for four PZT sensors is defined as an index w, which is adopted to determine whether the impact happens inside the region. When the impact source moves from the sub-region center towards the boundary, w gradually increases. To determine the range of w in the sub-area, structure finite element model needs to be developed to obtain the simulated strain responses of four sensors under the standard impact force, which is at the node in the sub-area or near the border. The w near the border is set to be the time lag threshold δ as the upper bound. If w is smaller than δ, PZT SA deems that the impact occurs in the area, else out.

The blackboard of DMA is replaced with shared variables which are adopted to store the subarea damage state "damage close to boundary" or "damage inside the subarea" and data of PZT SA. When a PZT SA detects a signal crossing the threshold of the digital trigger, it sends the impact event status and data to its blackboard unit in its DMA. The shared variable is set to be logic 1, and it indicates that the impact occurs in this subarea of PZT SA. If there is no impact event or the impact being in other regions, its shared variable is logic 0.

Once DMA finds that the agent's state in the blackboard is 1, then it could inquire whether the status of its neighboring PZT SA in the blackboard is 1, and if so, the impact occurs near the border between two PZT SAs, and otherwise, the impact occurs only in-house. Then DMA can extract the subarea damage data from the single PZT SA, or the boundary damage data from two PZT SAs.

3. 3. 2. Evaluation agent coordination

After DMA obtains the arrival times from WT SPA, it can respectively send the arrival times and the strain data to TL DEA and IAL DEA, and tell them the other part's addresses and IDs. Therefore, they can know the other part's blackboard layer in its SIMA, query the interesting information in the blackboard, determine whether to read the other part's or write its own blackboard layer and identify the impact location.

First of all, to shorten the computation time of IAL DEA and to fast generate an approximate result, a position threshold is introduced. It is defined as the supremum of the minimum of the strain error e for all finite element nodes, that is:

$$\sigma = \sup_p \min e = \sup_p \min \sum_{i=1}^{N} \left\| \varepsilon_i - \varepsilon_i^* \right\|_2^2 / \sum_{i=1}^{N} \left\| \varepsilon_i^* \right\|_2^2 \tag{5}$$

In the study, the improved IAL DEA random orderly traverses the finite element node in the structure and looks for the impact point which has $e < \sigma$. If it exists that $e < \sigma$ for some node, its location is deemed as the ideal impact point. The improved method may largely reduce the computation time of searching for all the finite element nodes, and reduce the scope of the solution.

The coordination process is shown in Fig. 10. It is assumed that the computation time of TL DEA and IAL DEA is t_{tr} and t_{tr}. The coordination principle is as follows.

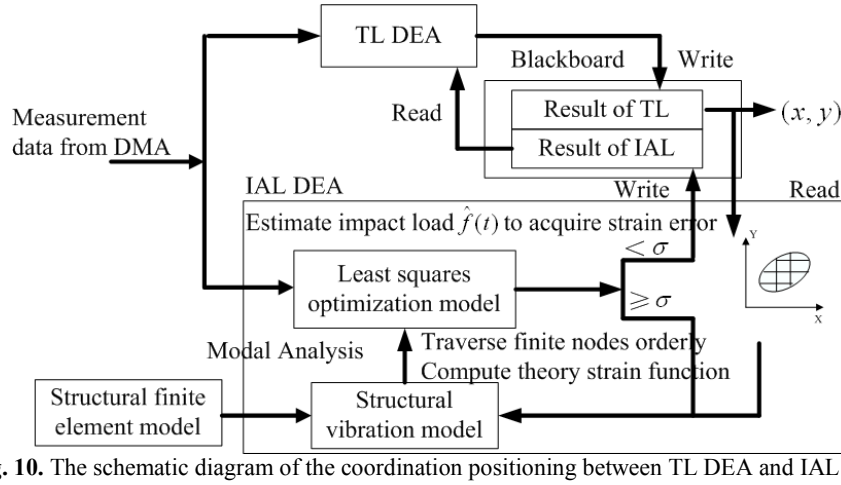

Fig. 10. The schematic diagram of the coordination positioning between TL DEA and IAL DEA

Firstly, the case of $t_{tr} \leq t_{in}$ is discussed because the computation speed of TL DEA is generally very fast. Once DMA notifies two evaluation agents, TL DEA chooses any three from four arrival times, and computes to obtain four impact points (x_1, y_1), (x_2, y_2), (x_3, y_3), (x_4, y_4). Since the arrival time and the propagating speed easily change due to

anisotropy, dispersion and noise, the location error could occur in the source location. Hence, the latitude and longitudinal coordinate of the impact location is deemed to be the binary random variable (*X*, *Y*). The four points are the samples of the source location, and are adopted to estimate the position with their mean vector and variance matrix, which are defined as $M=[m_x,m_y]^T$, $\Lambda = diag[\sigma_x^2,\sigma_y^2]$. Geometrically, the ideal impact point is in an elliptical district of the two-dimensional random variables space. The samples and the mean vector can be employed to obtain the covariance matrix, which is defined as $M=[m_x,m_y]^T$, $P=[\sigma_{ij}^2]=[E[(x_i-m_x)(y_i-m_y)]]$, where $E(\cdot)$ is the mathematical expectation. The variance matrix Λ is given by an orthogonal transformation of the covariance matrix *P* as:

$$P = V\Lambda V^T = [v_1,v_2]\begin{pmatrix}\sigma_x^2 & 0\\ 0 & \sigma_y^2\end{pmatrix}[v_1,v_2]^{\mathrm{T}} \tag{6}$$

where v_1, v_2 are the column vectors of the orthogonal matrix *V*. The four points and the estimation parameters M, Λ are published to the blackboard unit of TL DEA.

In reality the measured signals from sensors are often contaminated by measurement noise, and are easily affected by the dispersive properties of the plate wave generated by the impact. It is difficult to get accurate arrival time, and the positioning error of TL DEA is sometimes large. Hence, when IAL DEA queries and finds the updated result $M=[m_x,m_y]^T$ of the blackboard layer of TL DEA, it will first determine whether the value is reasonable. Here, the coordinate intervals of four sensors in sub-area are defined as $[x_{\min},x_{\max}]$, $[y_{\min},y_{\max}]$. If TL DEA's location result is to largely exceed 10 cm than the coordinate scope of the monitored subarea, IAL DEA will give up referring to the result, continuing to traverse the finite element nodes in the structure, and in turn optimizes a performance index *e* to obtain the import location.

If TL DEA result is in the coordinate scope of four sensors in the monitored subarea, IAL DEA can refer to the result. It deems that the ideal impact position probability distributes in the ellipse area, whose center is the mean $M=[m_x,m_y]^T$, and whose short and long axis are two times of variances σ_x, σ_y. It is assumed that the angle between the coordinate system *xOy* and $v_1O'v_2$ is θ, and the elliptic equation can be written in the form:

$$\frac{[\cos\theta(x-m_x)+\sin\theta(y-m_y)]^2}{(2\sigma_x)^2}+\frac{[-\sin\theta(x-m_x)+\cos\theta(y-m_y)]^2}{(2\sigma_y)^2}=1. \tag{7}$$

Thus, it only traverses some finite element nodes in the ellipse district and gets the impact position whose strain error *e* is less than position threshold σ. As a result, the most computation time is spent in the closest point search step, and it is to speed up the search process. At last, the optimal impact point is published to DMA. Then SIMA is notified to clear the blackboard layer of TL DEA.

Secondly, the case of $t_{tr} > t_{in}$ is given as follow. It is known that the number of the Chebyshev polynomial coefficients is properly chosen to be able to reduce unknown variables, and the regularization technology can be adopted to improve the ill-pose effects of the inversion. Therefore, the convergence is fast, and the computation time may be short. Otherwise, the structure nodes are traversed random orderly. Hence, there may exist that

$t_{tr} > t_{in}$ near the first traversed nodes at the beginning. Before TL DEA finishes the computation, IAL DEA releases the result (x_{in}, y_{in}) to its own blackboard layer in SIMA. When TL DEA inquiries the solution in the blackboard, it amends its four impact points as follows.

Let *S* denote the set of the impact points, that is:

$S = \{(x_1, y_1), (x_2, y_2), (x_3, y_3), (x_4, y_4), (x_{in}, y_{in})\}$,

Step 1: Give the mean $M^{'} = [m_x^{'}, m_y^{'}]^T$ of five points in *S*,

Step 2: Remove the furthest point from the mean in *S*, and have:

$$S^{'} = S - \max_{(x,y)\in S} \left\| [x, y]^T - [m_x^{'}, m_y^{'}]^T \right\|,$$

Step 3: Take the mean $M^{''} = [m_x^{''}, m_y^{''}]^T$ of the remaining four points in $S^{'}$ as the ultimate impact location.

The final result is published to DMA. Then SIMA is notified to clear the blackboard layer of IAL DEA.

If the damage happens in the sub-area, DMA passes the "damage inside the subarea" state and only one location result to CCRA. It directly sends its coordinate to UIA. If the damage occurs near the sub-region boundary, DMA waits and orderly accepts two results of DEAs for two neighboring PZT SAs, and notifies the "damage close to boundary" state and two locations to CCRA. CCRA knows the damage occurs close to the border, and sends two positions to CIFA. Since two positions are from two local coordinates of two adjacent agents, a coordinate transformation is needed. CIFA can finish the work, use the average to fusion two location results, and send the result to UIA.

4. Experiment validation

In order to have a better demonstration of the advantages of SHM MAS, two monitoring cases are also given. The first case is to monitor the impact source near the boundary between Subarea 1 and 2 or 5 to validate the blackboard coordination in data monitoring layer agents. The second case is the accuracy localization identification of the impact load in Subarea 5 to validate the blackboard coordination between the damage evaluation agents.

To monitor the impact location, the local and global coordinate systems are adopted for different evaluation methods as shown in Fig. 9. The local coordinate system X_nOY_n is adopted for TL DEA, in which *n* is number of the subarea, and the global coordinate system *XOY* is adopted for IAL DEA. The location errors are compared for the given impact locations to determine the effectiveness of MAS. The error is defined as the distance from the actual impact location (x_0, y_0) to the calculated location (x, y).

An impact hammer is utilized to replace an impact load. PZT sensors 1-9 layout is shown in Fig. 9. For the charge amplifier, its sensitivity coefficient is set to be 10.99 pC/unit, and the magnification is 1 mV/unit, and the bandwidth of its filter is 0-100 kHz. Digital trigger threshold is 0.5 V with the synchronous method. The number of its pre-acquisition points is 800, and the sampling frequency is 1 MHz, and the total measurement time is 0.012 s.

4. 1. Subarea boundary monitoring

To verify the effectiveness of the subarea boundary collaborative localization in the data monitoring layer, subarea 1, 2 and 5 is considered in Fig. 2. In SHM MAS, PZT SA 1, 2 and 5 and DMA are started up in the data monitoring layer and TL DEA is only started up in the damage diagnostic layer.

As shown in Fig. 9, the formula of coordination transformation between Subarea 1 and 2, 5, and between Subarea 1 and the global coordinate is easily obtained.

The acquired signal is as shown in Fig. 11. When a digital high-pass filter with cutoff frequency 10 kHz is adopted to filter the acquired signal, the impact signal can be obtained as shown in Fig. 11 (b).

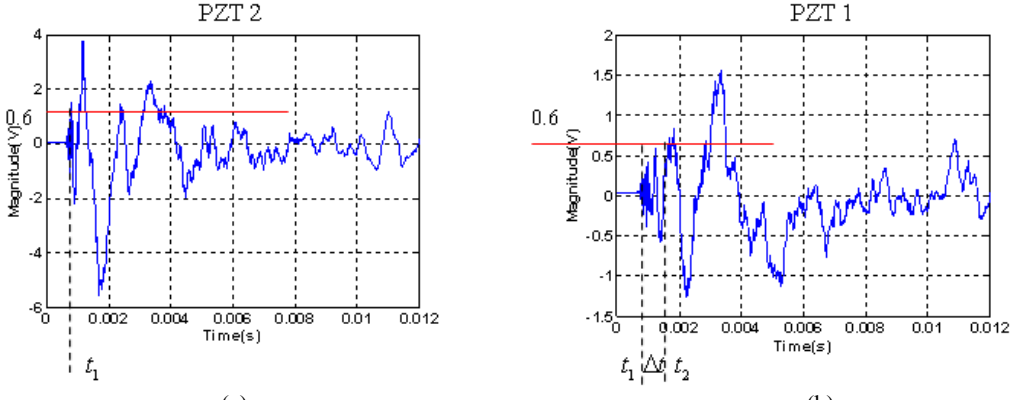

Fig. 11. The acquired signal of PZT sensor 1 and 2

Considering signal noise ratio, the threshold value of the threshold crossing method is set to be 0.6 V in Fig. 11. The upper bound 0.49 ms of w for PZT SA is set according to the finite element modeling analysis based on MSC Patran/Nastran software [20] and practical loading experiments. The fitted distribution of w in X_5OY_5 of Subarea 5 is shown in Fig. 12. With Fourier spectrum analysis, it is known that the main frequency generated by the impact hammer is about 20 kHz.

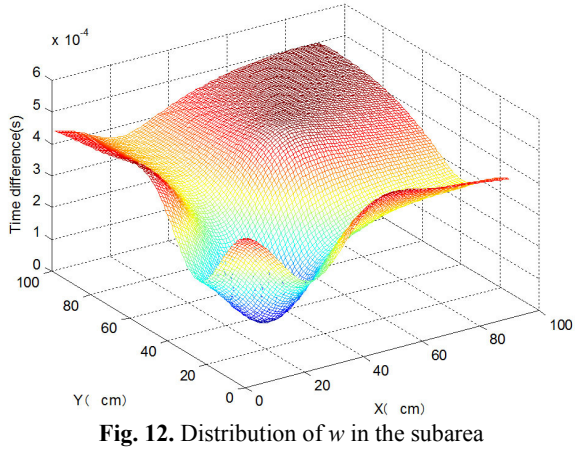

Fig. 12. Distribution of w in the subarea

Figure 13 provides the localization results of twelve impact points in the sub-region and near the boundary. Fig. 13 (a) and (b) indicate that the results in the subarea are better than the ones close to the boundary. Fig. 13 (a) reveals that for PZT SA 1, the localization results in the subarea are consistent with the actual ones, and its location errors are less than 2.0 cm, while the location errors near the boundary are generally greater than 3.0 cm. In addition, the location errors of some points near the border for PZT SA 2 and 5 are very large as shown in Fig. 13 (b).

The larger errors close to the boundary are due to the larger distance difference between the impact resource and four sensors. Four sensors acquire different Lamb wave modes, so the extracted arrival time error is very large; this is why the error near the boundary is larger. Due to the problem, the multi-agent blackboard coordination method is adopted in the boundary localization.

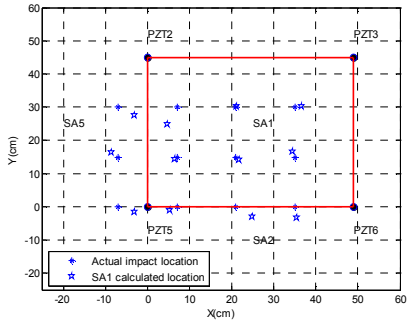

(a) SA1 calculated location

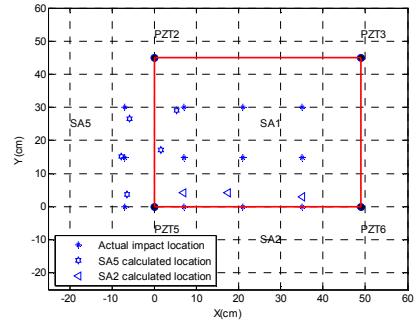

(b) SA2 and SA5 calculated location near boundary

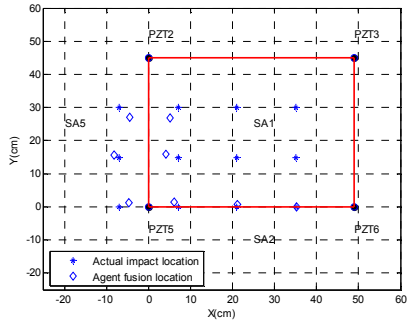

(c) Agent fusion location close to boundary

Fig. 13. Multi-agent coordination localization results for the subarea boundary

Figure 13 (c) illustrates localization results of fusing the distributed information from the strain data of PZT SA 1 and PZT SA 5 or 2. For the boundary points between PZT SA 1 and 5, the location errors are 3.8 cm, 1.4 cm, 2.5 cm, 3.7 cm, 3.1 cm and 1.8 cm. For the boundary points between PZT SA 1 and 2, the location errors are 1.8 cm, 0.6 cm and 0.2 cm. Most results are better than PZT SA 1's. In summary, the collaborative localization method is effective for the internal sub-region and, especially, the boundary.

4. 2. Coordination evaluation

To verify the effectiveness of the coordination localization between the evaluation agents in the damage diagnostic layer, Subarea 5 is considered in Fig. 14. In SHM MAS, PZT SA 5 is started up, and TL DEA and IAL DEA are only started up in the damage diagnostic layer. Seven experimental impact points in the plate are chosen and numbered in Fig. 14.

For IAL DEA, the finite element model of the large aluminum plate is also built using Patran/Nastran software. The region 70×60 cm^2 of interest in Fig. 14 is divided to the uniform meshes with 1×1 cm^2. Other region in plate is divided sparsely. There are 5960 plate elements in the model, which are the four-node non-coordination bending one based on the Kirchhoff

plate theory. The spectrum energy observed is mainly lower than 1 kHz. Consequently, the first 250 natural vibration modes of the structure are employed in the present study. Otherwise, when the first 45 Chebyshev basis functions are adopted, the impact force history can rapidly converge. Taking the precision of the inversion analysis into account, the acquiring signal is re-sampled with the interval 0.0001 s, and the discrete signal is composed of 120 points.

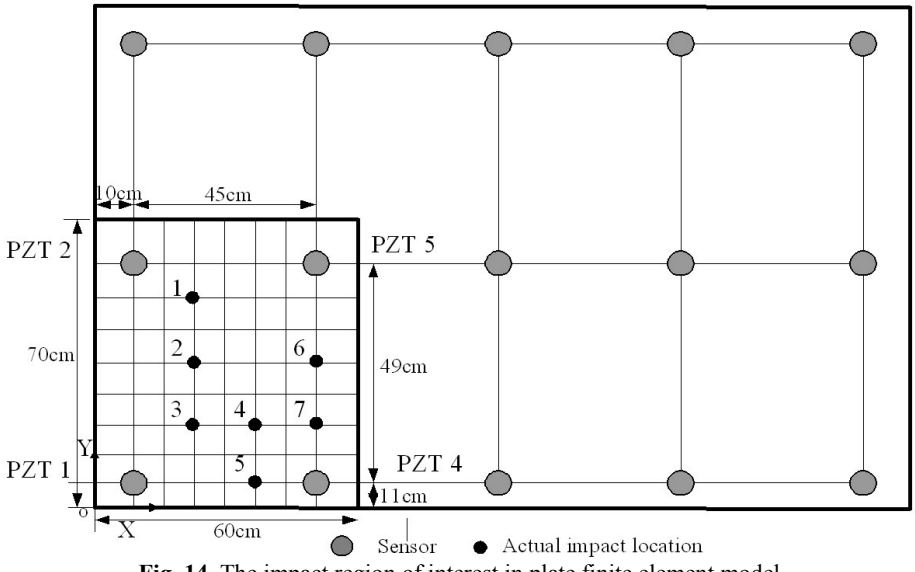

Fig. 14. The impact region of interest in plate finite element model

The actual impact location, the calculated location, the location error and the computation time of TL DEA and IAL DEA are given in Table 2. The coordination localization results between TL DEA and IAL DEA are also given in the Table.

Table 2. The location results of TL DEA, IAL DEA and the coordination between two agents

Impact location (Unit: cm)	Calculated location	Location error	Computation time (Unit: s)
1 (25, 53)	(25.6, 54.9)/(29, 47)/(25.6, 54.9)	2.0/7.2/2.0	1.6/33.4/2.5
2 (25, 39)	(24.7, 39.0)/(26, 40)/(25.0, 39.0)	0.3/1.4/0.0	1.6/36.7/2.6
3 (25, 25)	(24.5, 25.2)/(26, 28)/(25.0, 25.0)	0.5/3.2/0.0	1.5/45.8/2.3
4 (40, 25)	(40.4, 24.8)/(40, 22)/(41.0, 24.0)	0.4/3.0/1.4	1.7/53.5/2.5
5 (40, 11)	(-, -)/(40, 11)/(40.0, 11.0)	-/0.0/0.0	1.7/54.3/46.0
6 (55, 39)	(55.1, 39.5)/(59, 40)/(55.0, 39.0)	0.5/4.1/0.0	1.8/36.7/3.2
7 (55, 25)	(-, -)/(51, 23)/(51.0, 23.0)	-/4.5/4.5	1.7/60.3/55.0

The related results of identified impact locations are reported for TL DEA in Table 2. For seven impact positions, the identification time of TL DEA is about 1.6 s. The location error at Position 1 is 2.0 cm, and the ones at Positions 2, 3, and 4 are smaller than 0.5 cm. However, the calculated locations of Position 5 and 7 are far larger than the coordinate range of the 5th sub-region, so their calculated location and location error are represented by "-" in the Table. The corresponding location error of Position 6 is 0.5 cm. From these results it can be found that when the impact location is near the sub-region boundary, the identification accuracy of the impact position decreases and in the sub-region there is good agreement between the actual and the calculated location. The reason of the positioning inaccuracy on the border is the same as the one in Section 4.1.

The results of IAL DEA are given in Table 2. For Positions 1, 2, 3 and 4, the agent needs to traverse the finite element nodes in the whole subarea, so the identification time is from 33 s to 54 s, and the location error at Position 1 is 7.2 cm and smaller than 3.5 cm at the other three locations. For Positions 5, 6 and 7, the identification time is larger than 33 s and smaller than 60.5 s. But the corresponding location error at Position 5 is 0.0 cm, and the others are about 4.0 cm. It can be observed that the location errors are largest for Positions 1, 6 and 7. This may be mainly caused by the difference between the numerical model and experimental setup.

For the collaborative positioning between TL DEA and IAL DEA, its results are also provided in Table 2. In order to verify the effectiveness of the improved IAM DEA, it is assumed that the method not randomly traverses the finite element nodes (it traverses the structure sequentially). At Positions 1, 2, 3, 4, the location errors are 2.0 cm, 0.0 cm, 0.0 cm and 1.4 cm respectively. When the impact takes place at Position 1, IAL DEA traverses the nodes of the 5th sub-region from the top left corner by row in Fig. 14. Once the performance index e is less than σ, the agent deems that node is the actual impact position, whose identification time is 1.5 s and the location error is 7.2 cm. The position threshold σ is set to be 0.1850 as shown in Table 3. Then, IAL DEA publishes the result to the blackboard. When TL DEA finds the result, it amends its calculated four impact points, and discards the worse one in five points. The agent takes 2.5 s, and the location error is 2.0 cm.

Table 3. The selection of position threshold σ

Position threshold	1	2	3	4	5	6	7
σ	0.1847	0.1188	0.1034	0.1234	0.1418	0.1405	0.1577

For Positions 2, 3, 4, 6, TL DEA finishes task faster than IAL DEA. When IAL DEA finds TL DEA result in the blackboard, which are not to exceed the range of the sub-region coordinates, IAL DEA stops searching, establishes the elliptical region with the mean and 2 times variance of TL DEA calculated four points, traverses the region and rapidly converges to the optimal point. The location errors are 0.0 cm, 0.0 cm, 1.4 cm and 0.0 cm.

Take Position 2 as example, IAL DEA takes 4.7 s to obtain the coordinate (24.9 cm, 38.9 cm) in the blackboard, corresponding to the probability distribution elliptical area in Fig. 15. IAL DEA orderly traverses the nodes of the elliptical area, that is (24 cm, 39 cm), (25 cm, 39 cm), (25 cm, 38 cm), and spent 1.7 s to find the optimal point (24.9 cm, 38.9 cm), whose e is less than the threshold. Here the reconstructed impact history is as shown in Fig. 16, and the measured and the strain response evaluated using the numerical model for PZT sensor 1 are shown in Fig. 17. Wavelet transform result of the acquired signal is presented in Fig. 18.

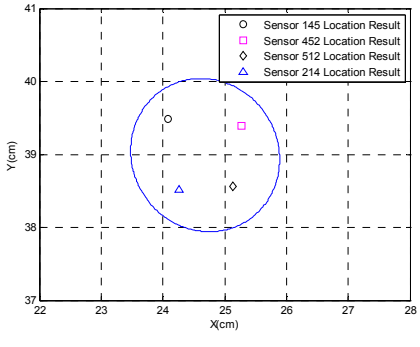

Fig. 15. The probability distribution elliptical region of triangulation positioning results at impact position 2

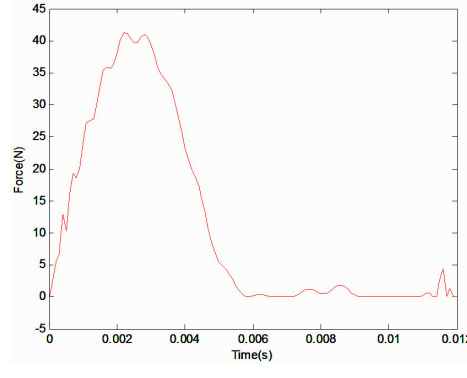

Fig. 16. The reconstruction impact force

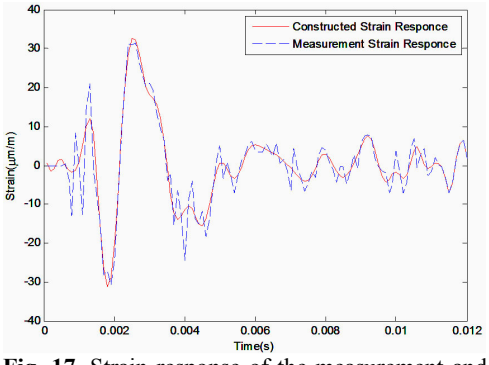

Fig. 17. Strain response of the measurement and reconstruction for PZT sensor 1

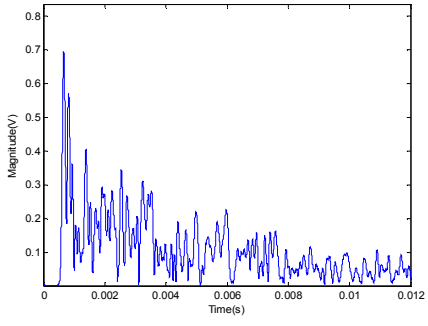

Fig. 18. Wavelet transform of the acquired signal for PZT sensor 1

When the impact occurs at Positions 5, 7, TL DEA firstly finishes the computation, and publishes the result to blackboard, but the result is far to exceed the coordination range of the monitored area. Hence, after IAL DEA finds it, it does not use the result and goes to traverse the other nodes to obtain the result. The location error is 0.0 cm and 4.5 cm.

In summary, the identification time of TL DEA is shorter than IAL DEA, but near the boundary the identification accuracy is lower. The identification time of IAL DEA is sometimes longer than TL DEA, but its location error is not large near the boundary, and larger than TL DEA for some points in the region. The coordination positioning between TL DEA and IAL DEA synthesizes their advantages. For the identification of the impact location in the area or near the boundary, it obtains the trade-off in both accuracy and computation time with the good robustness.

5. Conclusions

MAS is applied to integrate distributed sensors and different evaluations in order to give a fast and reliable impact location in practical large structures. The evaluation work in the large aerospace aluminum plate demonstrates that the advantages of MAS are as follows:

(1) The whole system can manage the sensor network to focus on the impact load in the each sub-region, especially on its boundary, and provide the effective information.

(2) Different evaluation methods can communicate, coordinate and refer to the shared results with each other for the impact positioning. Its result is more robust, effective and accurate.

(3) According to the subarea damage state, the evaluation results are fused to accurately estimate the impact location in the subarea, especially near the sub-region boundary. Through cooperation, the monitoring system efficiency can be improved.

This paper demonstrates that MAS can significantly improve the impact localization preciseness and real-time for large structures. In the future work, the validation work of multi-agent impact location on the large-scale composite material structure will be considered, and we will mainly study how to coordinate and speed up different evaluation methods in the anisotropic structure for the reliable impact localization.

Acknowledgements

This work was supported by European Union 7th Framework Programme International Cooperation Project (Grant No. FP7-PEOPLE-2010-IRSES-269202), Natural Science Foundation of China (Grant Nos. 60772072, 50830201 and 10872217), the Fundamental

Research Funds for the Central Universities and Funding of Jiangsu Innovation Program for Graduate Education (Grant No. CX10B_097Z).

References

[1] **Diamanti K., Soutis C.** Structural health monitoring techniques for aircraft composite structures. Progress in Aerospace Sciences, Vol. 46, Issue 8, 2010, p. 342-352.
[2] **Seydel R., Chang F. K.** Impact identification of stiffened composite panels: I. System development. Smart Materials and Structures, Vol. 10, Issue 2, 2001, p. 354-369.
[3] **Yuan S. F.** Structural Health Monitoring and Damage Control. Beijing: National Defense Industry Press, 2007.
[4] **Michael Wooldridge, Nicholas R. Jennings** Intelligent agents: theory and practice. Knowledge Engineering Review, Vol. 10, Issue 2, 1995, p. 115-152.
[5] **Stephen McArthur D. J., Strachan Scott M., Jahn Gordon** The design of a multi-agent transformer condition monitoring system. IEEE Transactions on Power Systems, Vol. 19, Issue 4, 2004, p. 1845-1852.
[6] **Lyell M. J., Krueger W., Zhang G., Xu R., Haynes L.** An agent-based approach to health monitoring systems applied to the ISS power system. The 45th AIAA Aerospace Sciences Meeting and Exhibit, Reno, Nevada, USA, 2008, p. 1-17.
[7] **Yew Seng Ng, Rajagopalan Srinivasan** Multi-agent based collaborative fault detection and identification in chemical processes. Engineering Applications of Artificial Intelligence, Vol. 23, Issue 6, 2010, p. 934-949.
[8] **Abbott David, Doyle Briony, Dunlop John and et al.** Development and Evaluation of Sensor Concepts for Ageless Aerospace Vehicles. NASA Technical Report NASA/CR-2002-211773, Langley Research Center, Hampton, Virginia, 2002.
[9] **Albert Esterline, Bhanu Gandluri, Mannur Sundaresan, Jagannathan Sankar** Verified models of multi-agent systems for vehicles health management. Smart Structures and Materials 2005: Modeling, Signal Processing and Control, Proceedings of SPIE, 5757, 2005.
[10] **Albert Esterline, Bhanu Gandluri, Mannur Sundaresan** Characterizing environmental information for monitoring agents. In Hinchey M. G. et al., Innovative Concepts for Autonomic and Agent-Based Systems, 2006, p. 74-85.
[11] **Yuan Shenfang, Lai Xiaosong, Zhao Xia, Xu Xin, Zhang Liang** Distributed structural health monitoring system based on smart wireless sensor and multi-agent technology. Smart Materials and Structures, Vol. 15, Issue 1, 2006, p. 1-8.
[12] **Zhao Xia, Yuan Shenfang, Yu Zhenhua** Designing strategy for multi-agent system based large structural health monitoring. Expert Systems with Applications, Vol. 34, Issue 2, 2008, p. 1154-1168.
[13] **Zhao Xia, Yuan Shenfang, Zhou Hengbao, Sun Hongbing, Qiu Lei** An evaluation on the multi-agent system based structural health monitoring for large scale structures. Expert Systems with Applications, Vol. 36, Issue 3, 2009, p. 4900-4914.
[14] **Jeong Hyunjo, Jang Young-Su** Wavelet analysis of plate wave propagation in composite laminates. Composite Structures, Vol. 49, Issue 4, 2000, p. 443-450.
[15] **Armaghan Salehian** Identifying the Location of a Sudden Damage in Composite Laminates Using Wavelet Approach. Worcester Polytechnic Institute, USA, 2003.
[16] **Ohkami Y., Tanaka H.** Estimation of impact force and its location exerted on spacecraft. Transactions of the Japan Society of Mechanical Engineering, Ser. C, 63C, 1997, p. 4246-4252.
[17] **Yen C.-S., Wu E.** On the inverse problem of rectangular plates subjected to elastic impact, Part I: Method development and numerical verification. Journal of Applied Mechanics, Transactions of the ASME, Vol. 62, Issue 3, 1995, p. 692-698.
[18] **Hu N., Fukunaga H., Matsumoto S., Yan B., Peng X. H.** An efficient approach for identifing impact force using embedded piezoelectric sensors. International Journal of Impact Engineering, Vol. 34, 2007, p. 1258-1271.
[19] **Corkill Daniel D.** Blackboard systems. AI Expert, Vol. 6, Issue 9, 1991, p. 40-47.
[20] MSC Software Corporation. MSC Nastran Quick Reference Guide, 2001.